DOI: 10.1002/zaac.201000279

Four New Compounds Based on Terephthalate and 2-(4-Pyridyl)benzimidazole Ligands

Chang-Kun Xia,[a,b] Yun-Long Wu,[a] and Ji-Min Xie*[a]

Keywords: Benzimidazoles; Terephthalates; Cobalt; Nickel; Zinc; Magnetic properties

Abstract. Four new compounds based on H_2BDC and PyBIm [H_2BDC = 1,4-benzenedicarboxylatic acid, PyBIm = 2-(4-pyridyl)benzimidazole], $(PyBIm)(H_2BDC)_{0.5}$ (**1**), $Co(PyBIm)_2(HBDC)(BDC)_{0.5}$ (**2**), $Ni(PyBIm)_2(HBDC)(BDC)_{0.5}$ (**3**), and $Zn(BDC)(PyBIm)\cdot H_2O$ (**4**), were synthesized by hydrothermal methods and characterized by X-ray diffraction. Compound **1** contains two types of hydrogen bonding N–H···N and O–H···N, which connect the molecules into a two-dimensional (2D) layer. Complex **2** crystallizes isostructural to **3** in triclinic space group $P\bar{1}$, in 1D chains. The hydrogen-bonding interactions between uncoordinated N, N–H and COOH groups in **2** connect the 1D chains into a 2D layer. Complex **4** displays a 1D structure, which is finally extended to a 3D supramolecular framework by hydrogen bonding and π–π packing interactions. The magnetic properties of compounds **2** and **3** were studied as well.

Introduction

The unique strength, direction, and complementarity of non-covalent interactions such as hydrogen bonding and π···π interactions play a central role in the creation of molecular architectures for molecular self-assembly and molecular recognition in chemical, physical, and biological science.[1] The benzimidazole and its ramification with abundant non-coordinating N–H groups provide a good choice for studying hydrogen-bonding interactions.[2] Among the benzimidazole deviates, the 2-(4-pyridyl)benzimidazole (PyBIm) with three N donors can act as a good candidate to construct metal-organic frameworks, moreover, the N–H group plays an important role in formation of the metal-organic complexes. When PyBIm is in neutral form, the ligand displays monodentate[3] or bidentate[4] coordination modes (Scheme 1). In the case of the monodentate mode, the imino nitrogen atom (N_{py}) from pyridyl ring directly coordinates with the metal ions, whereas the N–H group and the imino nitrogen atom (N_{BIm}) from the BIm ring behave as hydrogen bonding donor (H–D) and acceptor (H–A), respectively. In the case of the bidentate mode, the ligand acts as bridge to join two metal ions with two imino nitrogen atoms from BIm and pyridyl rings, whereas the N–H group acts as H–D. Therefore, the PyBIm ligand provides in both coordination modes weak interaction sites for the construction of supramolecular assemblies. When PyBIm is deprotonated the ligand displays a tridentate coordination mode[5] (Scheme 1).

Recently, we synthesized a series of metal-organic complexes with the PyBIm ligand, such as $[Ag_2(PyBIm)_2(H_2O)_2]SO_4\cdot H_2O$, $[Ag_3(PyBIm)_3(\mu_2\text{-}SO_4)(HSO_4)]\cdot 3H_2O$, and $[Ag_2(PyBIm)_2(\mu_2\text{-}SO_4)]\cdot 4H_2O$ [4d], $[Ag(PyBIm)(H_2O)]NO_3$.[4a] In these complexes, the PyBIm ligand adopts bidentate coordination modes, and the N–H group of BIm does not coordinate to the metal ions, however, its hydrogen bonding interactions have important influence on the packing of the complexes. As part of our continuing investigation on this type of PyBIm complexes, we herein report four new compounds based on H_2BDC (1,4-benzenedicarboxylatic acid) and PyBIm ligands, namely, $(PyBIm)(H_2BDC)_{0.5}$ (**1**), $Co(PyBIm)_2(HBDC)(BDC)_{0.5}$ (**2**), $Ni(PyBIm)_2(HBDC)(BDC)_{0.5}$ (**3**), and $Zn(BDC)(PyBIm)\cdot H_2O$ (**4**).

Experimental Section

Materials and General Methods

The ligand 2-(4-pyridyl)benzimidazole (ByBIm) was synthesized according to the procedure reported by *Alcade* et al..[6] Other reagents and solvents employed were commercially available and used without further purification. Elemental analyses were carried out with an EA1110 CHNS-0 CE element analyzer and the IR spectra (KBr pellets) were recorded with a Nicolet Magna 750 FT-IR spectrometer in the range 400–4000 cm^{-1}. Thermogravimetric analyses (TGA) were performed with a Netzsch STA-499C thermoanalyzer under nitrogen (30–800 °C) at a heating rate of 10 $°C\cdot min^{-1}$. Variable temperature magnetic susceptibilities were measured with a model CF-1 superconducting extracting sample magnetometer; the powdered samples were kept in the capsule for weighing.

Syntheses of the Compounds

$[(PyBIm)(H_2BDC)_{0.5}]$ (1): A solution of $Mn(CH_3COO)_2\cdot 4H_2O$ (0.16 g, 0.64 mmol), PyBIm (0.24 g, 1.22 mmol), 1,4-H_2BDC acid

---

* Prof. Dr. J.-M. Xie
Fax: +86-511-88791800
E-Mail: jsuxie@163.com
[a] School of Chemistry and Chemical Engineering
Jiangsu University
Zhenjiang, 212013, P. R. China
[b] State Key Laboratory of Coordination Chemistry
Nanjing University
Nanjing, 210093, P. R. China

Supporting information for this article is available on the WWW under **http://dx.doi.org/10.1002/zaac.201000279** or from the author.

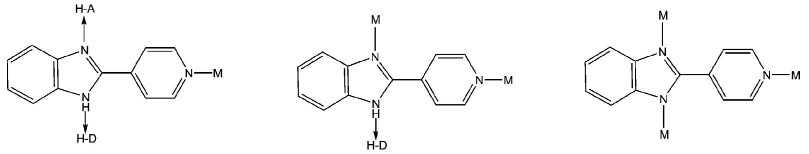

Scheme 1. Three types of coordination modes for the PyBim ligands.

(0.102 g, 0.61 mmol), and H_2O (15 mL) was stirred under ambient conditions. Afterwards, the mixture was sealed in a Teflon-lined steel vessel and heated at 160 °C for 5 days. After slow cooling to room temperature, the resulting product was recovered by filtration, washed with distilled water and dried in air (Yield 80 %). $C_{16}H_{12}N_3O_2$: calcd. C 69.06; N 15.10; H 4.35 %; found: C 69.13; N 14.87; H 4.74 %. **IR** (KBr): $\tilde{\nu}$ = 3455 s, 1854 m, 1695 s, 1613 s, 1534 m, 1505 m, 1447 w, 1433 s, 1372 m, 1314 s, 1277 s, 1210 m, 1131 m, 1060 s, 1014 s, 970 s, 879 m, 842 s, 772 s, 750 s, 723 s, 696 m, 616 w, 563 m, 481 s cm^{-1}.

Co(PyBIm)$_2$(HBDC)(BDC)$_{0.5}$ (2): A solution of $CoCl_2·4H_2O$ (0.152 g, 0.64 mmol), PyBIm (0.24 g, 1.22 mmol), 1,4-H_2BDC acid (0.160 g, 0.96 mmol), NaOH (0.022 g, 0.55 mmol) and H_2O (15 mL) was stirred under ambient conditions. Afterwards, the mixture was sealed in a Teflon-lined steel vessel and heated at 130 °C for 5 days. After slow cooling to room temperature, the resulting product was recovered by filtration, washed with distilled water and dried in air (Yield 85 %). $C_{36}H_{25}CoN_6O_6$: calcd. C, 62.08; N, 12.06; H, 3.62 %; found: C, 61.79; N, 12.32; H, 3.91 %. **IR** (KBr): $\tilde{\nu}$ = 3422 s, 3196 s, 1932 m, 1674 s, 1613 s, 1563 s, 1550 m, 1507 s, 1430 s, 1408 s, 1316 m, 1273 m, 1234 m, 1214 m, 1014 s, 958 m, 884 m, 842 s, 814 m, 789 s, 739 s, 698 s, 682 s, 532 m cm^{-1}.

Ni(PyBIm)$_2$(HBDC)(BDC)$_{0.5}$ (3): Complex **3** was synthesized in an analogous procedure to **2**, except $NiCl_2·4H_2O$ (0.144 g, 0.64 mmol) was used instead of $CoCl_2·4H_2O$ (Yield 80 %). $C_{36}H_{25}NiN_6O_6$: calcd. C, 62.10; N, 12.07; H, 3.62 %; found: C, 61.79; N, 12.09; H, 4.04 %. **IR** (KBr): $\tilde{\nu}$ = 3424 s, 3195 s, 1932 m, 1672 s, 1614 s, 1567 s, 1542 m, 1508 s, 1430 s, 1406 s, 1315 m, 1258 m, 1258 m, 1214 m, 1017 s, 957 m, 884 m, 845 s, 814 m, 788 s, 740 s, 701 m, 682 s, 532 m cm^{-1}.

Zn(PyBIm)(BDC)·H$_2$O (4): A solution of $ZnCl_2·4H_2O$ (0.137 g, 1.00 mmol), PyBIm (0.195 g, 1.00 mmol), 1,4-H_2BDC acid (0.166 g, 1.00 mmol), NaOH (0.034 g, 0.85 mmol) and H_2O (15 mL) was stirred under ambient condition. Afterwards, the mixture was sealed in a Teflon-lined steel vessel and heated at 130 °C for 5 days. After slow cooling to room temperature, the resulting product was recovered by filtration and washed with distilled water and dried in air (Yield 90 %). $C_{20}H_{15}N_3O_5Zn$: calcd. C, 54.26; N, 9.49; H, 3.41 %; found: C, 54.62; N, 9.55; H, 3.88 %. **IR** (KBr): $\tilde{\nu}$ = 3451 s, 3052 s, 1869 m, 1614 s, 1563 w, 1536 m, 1500 m, 1478 m, 1448 w, 1371 m, 1277 s, 1143 m, 1130 m, 1060 s, 1015 s, 970 s, 879 m, 842 s, 771 m, 745 s, 705 m, 695 m, 593 m, 563 m cm^{-1}.

X-ray Crystallography

Suitable single crystals of **1**–**4** were carefully selected under an optical microscope and glued to thin glass fibers. The diffraction data were collected with a Siemens Smart CCD diffractometer with graphite-monochromated Mo-K_α radiation (λ = 0.71073 Å) at 293 K. An empirical absorption correction was applied using the SADABS program.[7] The structures were solved by direct methods and refined by full-matrix least-squares methods on F^2 by using the SHELXTL-97 program package.[8] The hydrogen atoms were generated geometrically except for water molecules. Crystallographic data are summarized in Table 1. Selected bond lengths and angles are listed in Table 2.

Crystallographic data for the structural analysis have been deposited with the Cambridge Crystallographic Data Centre, reference numbers CCDC-773909, -773910, -773911, and -773912 for compounds **1**–**4**. Copies of this data may be obtained from The Director, CCDC, 12 Union Road, CB2 1EZ, UK (Fax: +44-1233-336033; E-Mail: deposit@ccdc.cam.ac.uk or www: http:// www.ccdc.cam.ac.uk.)

Supporting Information (see footnote on the first page of this article): TGA and DSC traces of compounds **1**–**4**. Inverse susceptibility with linear regression based upon Curie–Weiss law for complexes **2** and **3**.

Results and Discussion

Syntheses

Complexes **2**–**4** were synthesized with transition metal chlorides in hydrothermal reaction condition, respectively. However, a series of parallel experiments show that when the metal chlorides were replaced with the corresponding metal acetates, the complexes could not be obtained, which may be due to the influence of CH_3COO^-. It is worthwhile to note that, more interestingly, the organic compound **1** was isolated from the similar reaction condition with $Mn(CH_3COO)_2·4H_2O$ as initial reagent. However, if the synthesis was carried out under the same reaction conditions but in absence of Mn^{2+} or Co^{2+} ions, no compound **1** could be obtained, which suggests that the presence of metal ions is important to obtain the structure although the role of the metal ions in the system remains unclear.

Thermal Properties

Compound **1** does not show apparent weight losses up to 250 °C. A sharp weight loss occurs between 250–360 °C, which displays the decomposing of the overall molecule. Because no coordination or crystal water molecules are present in the complexes **2** and **3**, the two complexes are rather stable and have no weight losses up to 370 °C. Complex **4** loses its coordination water in the range of 45–150 °C, the observed weight loss is 3.98 %, which is in accordance with the calculated weight loss (4.07 %).

Crystal Structures

Compound **1** crystallizes in orthorhombic space group *Pbca*. As shown in Figure 1, in the molecule structure the PyBIm co-

Table 1. Crystal data and structure refinement parameters for compounds **1**–**4**.

	1	**2**	**3**	**4**
Formula	$C_{16}H_{12}N_3O_2$	$C_{36}H_{25}CoN_6O_6$	$C_{36}H_{25}NiN_6O_6$	$C_{20}H_{15}ZnN_3O_5$
Molecular mass	278.29	696.55	696.33	442.72
Crystal system	Orthorhombic	Triclinic	Triclinic	Triclinic
Space group	*Pbca*	$P\bar{1}$	$P\bar{1}$	$P\bar{1}$
a /Å	7.4475(3)	9.6096(13)	9.651(5)	8.7966(10)
b /Å	10.2079(5)	10.4902(11)	10.462(5)	9.0647(10)
c /Å	35.2470(18)	15.864(2)	15.876(9)	12.7578(18)
α /°	90	95.121(3)	95.288(17)	102.534(5)
β /°	90	107.158(7)	107.099(9)	106.203(3)
γ /°	90	94.574(4)	94.983(11)	90.450(5)
V /Å^3	2679.6(2)	1512.4(3)	1514.7(14)	951.1(2)
Z	8	2	2	2
T /K	293(2)	293(2)	293(2)	293(2)
D_{calc} /g·cm^{-3}	1.380	1.530	1.527	1.546
F(000)	1160	716	718	452
Reflections collected	15788	11852	11827	7425
Independent reflections	3063	6862	6850	4311
Data/restrain/parameters	3063 / 0 / 194	6862 / 0 / 446	6850 / 0 / 446	4311 / 0 / 270
Goodness-of-fit on F^2	1.148	1.115	1.106	1.064
Final R indices [$I > 2\sigma(I)$]	0.0502, 0.1194	0.0641, 0.1181	0.0702, 0.1227	0.0452, 0.1138
R indices (all data)	0.0527, 0.1211	0.0940, 0.1360	0.1106, 0.1442	0.0550, 0.1210
Electron density	0.222, –0.219	0.478, –0.436	0.335, –0.494	1.188, –0.521

Table 2. Selected bond lengths /Å and angles /° for compounds **1**–**4**.

1			
C(13)–O(1)	1.309(2)	C(13)–O(2)	1.208(2)
C(1)–N(1)	1.337(2)	C(5)–N(1)	1.333(2)
C(6)–N(2)	1.323(2)	C(6)–N(3)	1.364(2)
2			
Co(1)–O(1)	1.995(2)	Co(1)–O(2)	2.035(2)
Co(1)–O(5)	2.167(2)	Co(1)–O(6)	2.154(2)
Co(1)–N(1)	2.172(3)	Co(1)–N(4)	2.171(3)
O(2)–Co(1)–O(6)	89.57(9)	O(2)–Co(1)–O(5)	150.24(9)
O(2)–Co(1)–N(1)	90.05(1)	O(6)–Co(1)–O(5)	60.86(8)
O(5)–Co(1)–N(1)	94.66(1)	O(2)–Co(1)–N(4)	87.84(1)
O(6)–Co(1)–N(1)	93.27(1)	O(5)–Co(1)–N(4)	88.26(1)
N(4)–Co(1)–N(1)	176.96(1)	O(6)–Co(1)–N(4)	88.89(1)
3			
Ni(1)–O(1)	2.021(3)	Ni(1)–O(2)	2.015(3)
Ni(1)–O(5)	2.141(3)	Ni(1)–O(6)	2.107(3)
Ni(1)–N(1)	2.114(3)	Ni(1)–N(4)	2.111(3)
O(1)–Ni(1)–O(6)	154.74(1)	O(1)–Ni(1)–O(5)	92.72(1)
O(1)–Ni(1)–N(1)	92.83(1)	O(5)–Ni(1)–O(6)	62.35(1)
O(5)–Ni(1)–N(1)	94.29(1)	O(1)–Ni(1)–N(4)	85.83(1)
N(1)–Ni(1)–O(6)	93.05(1)	O(5)–Ni(1)–N(4)	88.25(1)
N(1)–Ni(1)–N(4)	177.19(1)	N(4)–Ni(1)–O(6)	89.20(1)
4			
Zn(1)–O(1)	1.932(2)	Zn(1)–O(3)	1.930(2)
Zn(1)–O(1W)	1.943(3)	Zn(1)–N(1)	2.049(3)
O(3)–Zn(1)–O(1)	107.87(9)	O(1)–Zn(1)–O(1 W)	100.96(1)
O(1)–Zn(1)–N(1)	106.33(1)	O(3)–Zn(1)–O(1 W)	125.14(1)
O(1W)–Zn(1)–N(1)	106.18(1)	O(3)–Zn(1)–N(1)	108.86(1)

crystallizes with H_2BDC in 2:1 ratio. The dihedral angle between the pyridyl and H_2BDC rings amounts 9.2°, whereas the angle between benzimidazoyl and pyridyl rings is 26.2°, respectively. There are two types of hydrogen bonding N–H···**N** and O–H···**N**. The neutral PyBIm molecules are linked by N3–H3A···**N**2^{i} (symmetry code i: –x+1/2, y–1/2, z) interactions to a 1D chain with a N–H···**N** distance of 2.944(2) Å and a N–H···N bond angle of 155.2° (Figure 2). Complex **4** crystallizes in triclinic space group $P\bar{1}$. As sTo the best of our knowledge, this type of self-complementary N–H···N hydrogen bonds is quite rare.[9] The chains are further linked by O1–H1B···N1^{ii} interactions (symmetry code ii: *x*–1, *y*, *z*) to a 2D "zigzag" sheet with an O–H···N distance of 2.654(2) Å and an O–H···N bond angle of 174(2)° (Figure 3). It is more interesting that the "zigzag" sheets are interpenetrating to form a 2D layer-like structure with ca. 16 Å thickness (Figure 4).

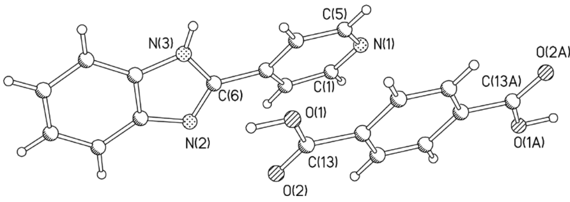

Figure 1. Molecular structure of compound **1**.

Complex **2** crystallizes in triclinic space group $P\bar{1}$, containing a crystallographically independent cobalt(II) atom [CoN_2O_4] as coordination center. As shown in Figure 5, in the cobalt atom is coordinated by four oxygen and two nitrogen donors in a distorted octahedral arrangement, with two oxygen atoms from chelating bis-bidentate carboxyl groups (Co1–O5 2.167(2) Å; Co1–O6 2.154(2) Å) and two oxygen atoms from two bridging bidentate carboxyl groups (Co1–O1A 1.995(2) Å; Co1–O2 2.035(2) Å). The O1A, O2, O5, and O6 atoms are almost coplanar with a mean deviation of 0.001 Å. The axial positions of the octahedral arrangement are completed by two nitrogen atoms from the terminal PyBIm ligands (Co1–N1 2.172(3) Å; Co1–N4 2.171(3) Å). In the structure of **2**, two cobalt(II) coordination units ([CoN_2O_4]) are linked together by two carboxyl groups of two terminal $HBDC^-$ ligands, forming an eight-membered ring (–Co1–O1A–C1A–O2A–Co1A–O1–C1–O2–) with a mean deviation of 0.1162 Å. The Co···Co separation amounts to 4.106 Å, which is obviously larger than that in the similar eight-membered ring in the dinuclear cobalt complex $Co_2(1,4\text{-}H_2BDC_2(dabco))]\cdot 4DMF\cdot H_2O$ (Co···Co = 2.684 Å).[10]

In complex **2**, the terephthalate anions exist in two different coordination modes ($HBCD^-$ and BCD^{2-}). The $HBCD^-$ anion, as terminal ligand, coordinates to two cobalt atoms (Co1 and Co1A) and employs its two carboxyl oxygen atoms (O1 and O1A) in a *syn*-*syn* mode. In contrast to the $HBCD^-$ anion, the BCD^{2-} anion acts as bridging ligand with bis-chelating mode, it connects the metal coordination units $[CoN_2O_4]_2$ into a one-dimensional chain (Figure 6).

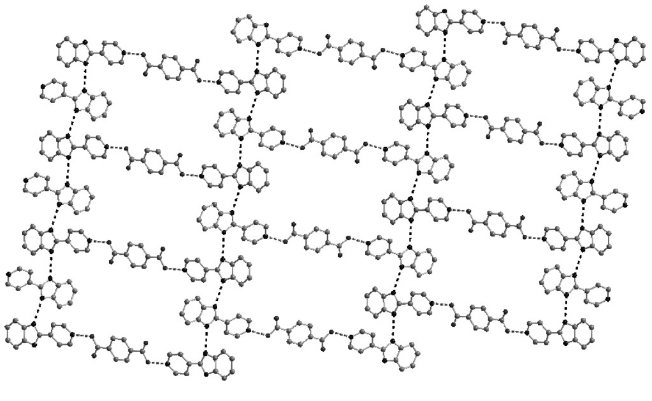

Figure 3. 2D "zigzag" sheet formed by N–H···N and O–H···N interactions.

It is noteworthy that weak interactions exist among the molecules of **2**. The hydrogen bonding interactions are formed between the non-coordinated carboxyl groups (COOH) of terephthalate ligands and the nitrogen heterocyclic rings of 2-(4-pyridyl)benzimidazole) ligands. The O4–H4B···N5^{iii} (symmetry code iii: –*x*+1, –*y*+2, –*z*+1) distance is 2.669(4) Å with a corresponding bond angle of 173°, whereas the N3–H3A···O3^{iv} (symmetry code iv: *x*–1, *y*–1, *z*) distance amounts to 2.801(4) Å with a bond angle of 169.8° (Figure 7). The overall structure displays a two-dimensional sheet formed by hydrogen bonding with windows of 11.66 Å × 12.94 Å (Figure 8). On the other hand, π–π stacking interactions of the aromatic rings of PyBIm ligands exist in the one-dimensional chain with face-to-face distances of 3.888–4.006 Å and dihedral angles of 6.1–18.3° for pair of rings.

Complex **3** crystallizes isostructural to complex **2**. We know that the ionic radius of Ni^{II} is 0.83 Å, which is slight shorter than that of Co^{II} (0.89 Å). So the distances of Ni–O and Ni–N are somewhat shorter than the corresponding bond lengths of **2** [Ni1–O1 2.021(3), Ni1–O2 2.015(3), Ni1–O5 2.141(3), Ni1–O6 2.107(3), Ni1–N1 2.114(3), and Ni1–N4 2.111(3) Å]. The Ni···Ni separation is 4.255 Å in the two nickel(II) coordination units ($[NiN_2O_4]_2$), and the hydrogen bonding interactions as well as π–π stacking interactions are similar to those of the complex **2**.

Complex **4** crystallizes in triclinic space group $P\bar{1}$. As shown in Figure 9, the zinc atom is tetracoordinated by two oxygen atoms (O1 and O3) from two monodentate carboxyl groups and one nitrogen atom (N1) from the terminal PyBIm ligand and one water molecule (O1W), forming a slightly distorted tetrahedral coordination unit [$ZnNO_3$]. The Zn1–O distances

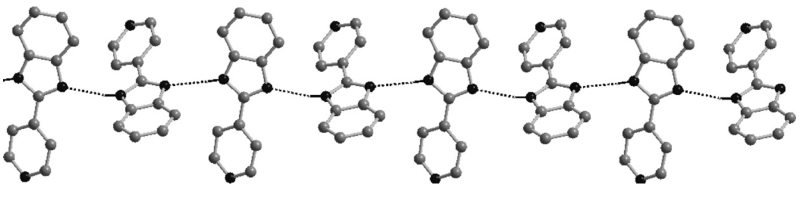

Figure 2. 1D PyBIm chain formed by N–H···N hydrogen bonding (dashed line).

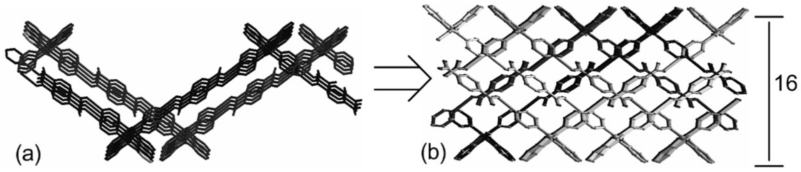

Figure 4. (a) Interpenetration of “zigzag” sheets. (b) 2D layer-like structure formed by the interpenetration of “zigzag” sheets.

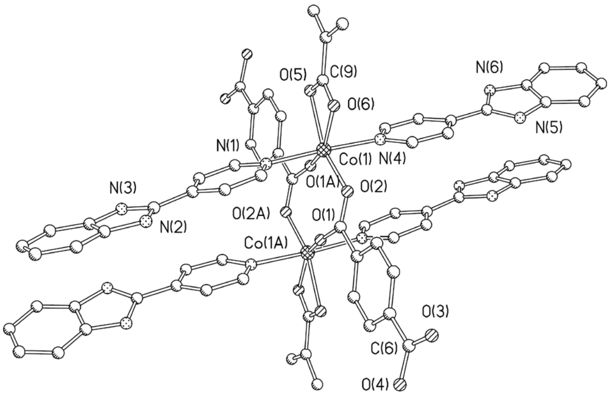

Figure 5. Locally expanded unit in complex **2**. Hydrogen atoms were omitted for clarity.

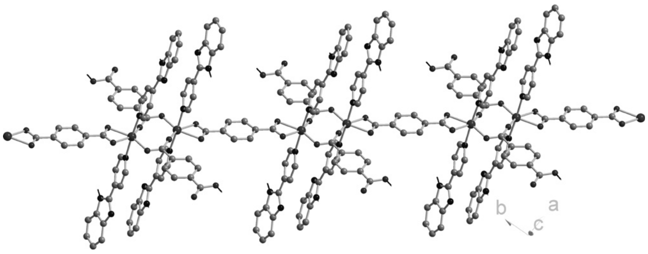

Figure 6. 1D polymeric chain formed by dimetal units in complex **2**.

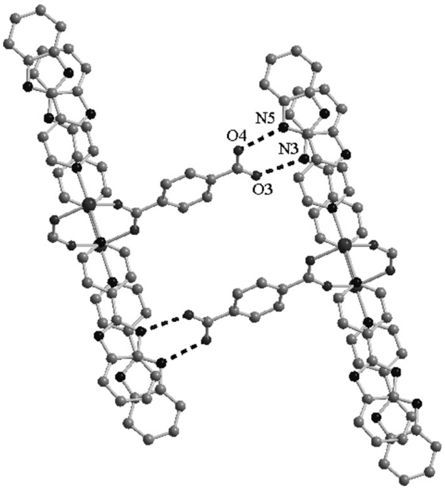

Figure 7. Hydrogen bonding interactions formed between the non-coordinated carboxyl groups (COOH) and the nitrogen heterocyclic rings.

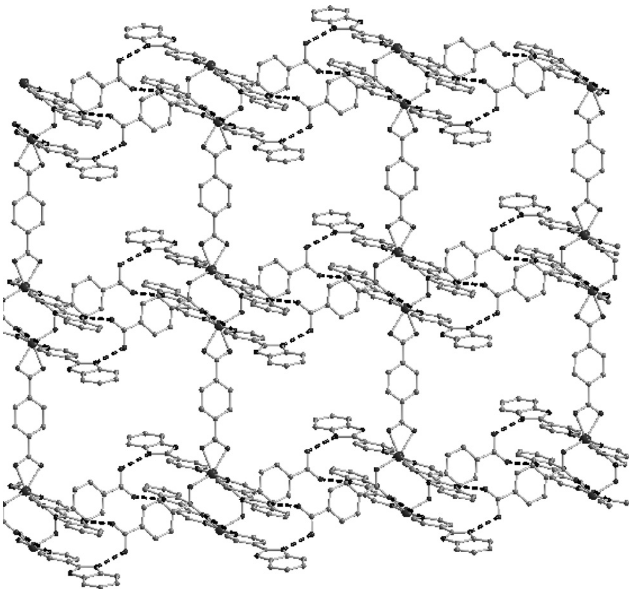

Figure 8. 2D sheet formed by the hydrogen bonding with windows of 11.66 Å × 12.94 Å.

amount to 1.932(2), 1.930(2), and 1.943(3) Å, and the Zn1–N1 distance is 2.049(3) Å. The O–Zn–O bond angles are 100.96(10), 107.87(9) and 125.1(1)°, and the N–Zn–O angles are 106.2(1), 106.33(10), and 108.86(10)°, respectively.

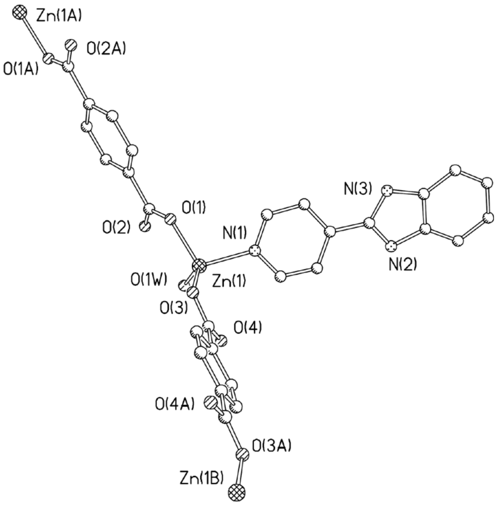

Figure 9. Locally expanded unit of complex **4**.

Like in complex **2**, the PyBIm molecule in **4** acts as a terminal ligand, which coordinates to the metal atom through a ni-

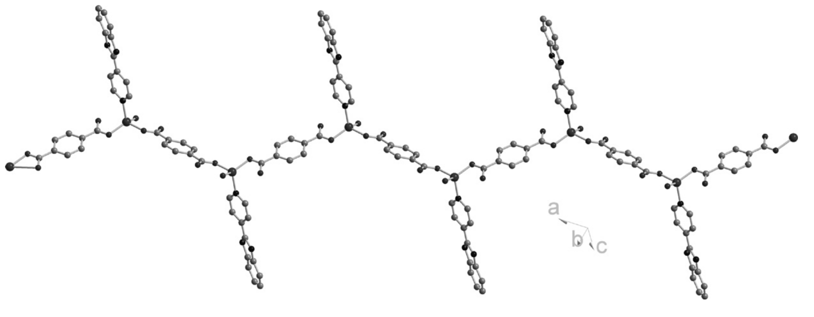

Figure 10. View of the 1D "zigzag" chain in complex **4**.

trogen atom, whereas the BDC^{2-} anion in **4** adopts a monodentate μ$_2$-bridging coordination mode, which is different to that in **2**. The coordination units [ZnNO$_3$] are connected by BDC^{2-} anions into a one-dimensional "zigzag" chain with a Zn···Zn separation of 11.09 Å (Figure 10). Hydrogen bonding interactions exist in the zigzag chains, and connect the chains into a 2D sheet (Figure 11) with a O1W–H1C···N2^{v} (symmetry code v: $-x+1$, $-y+2$, $-z+2$) distance of 2.668(3) Å and a bond angle of 170(5)°. Moreover, the sheets are further joined by π–π packing interactions (Figure 12) to form a three-dimensional framework (Figure 13), in which the interpenetrating aromatic rings are parallel to each other with face-to-face distances of 3.858(9) Å.

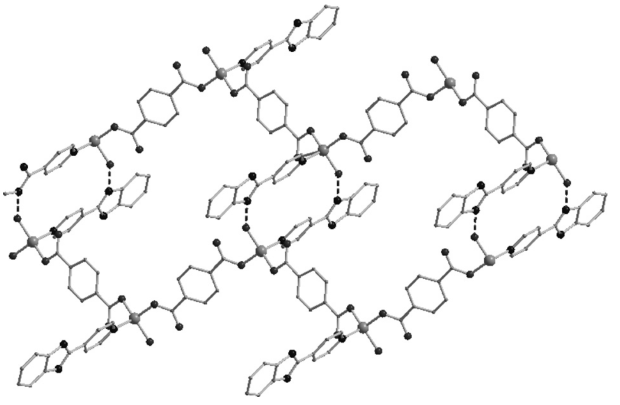

Figure 11. 2D sheet formed by hydrogen bonding interactions in complex **4**.

In the structures of complexes **2**–**4**, the PyBIm molecule only acts as the monodentate terminal ligand, different to other reported structures where it shows bi- or tridentate coordination [4, 5]. This may be ascribed to the employment of the terephthalate ligand, which has a strong bridging function and shows preferential coordination. Compared to the oxygen atoms of the terephthalate ligand, the N$_{\mathrm{BIm}}$ atoms have stronger steric hindrance. So, PyBIm preferentially adopts a terminal coordination mode using the N$_{\mathrm{py}}$ atom with weaker steric hindrance. On the other hand, the different hydrothermal reaction conditions may also be important to the difference of the coordination modes for PyBIm. Therefore, studying how to control the reaction conditions to carry out target-directed synthesis remains an important and active subject.

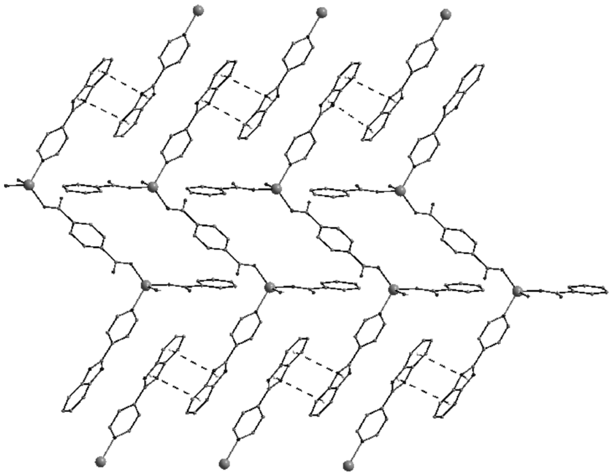

Figure 12. π–π Packing interactions in complex **4**.

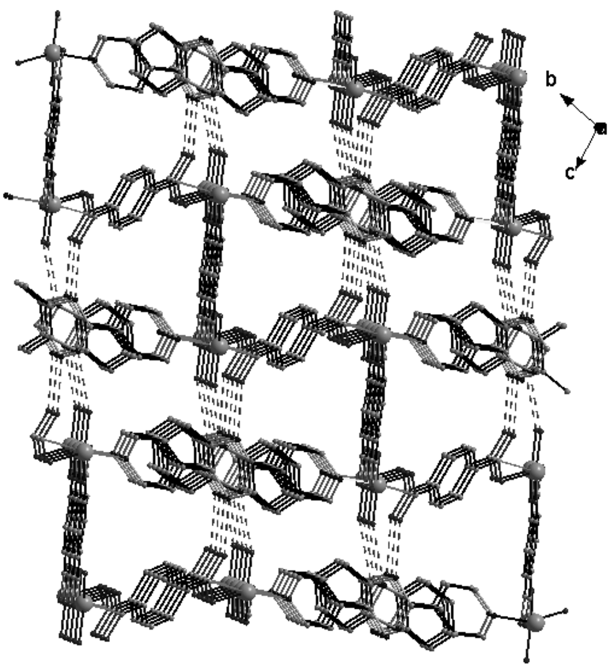

Figure 13. 3D framework formed by hydrogen bonding and π–π packing interactions.

Magnetic Properties

The temperature-dependent magnetic susceptibilities of complexes **2** and **3** were measured from 2 to 300 K. For complex **2**, the μ_{eff} value (per Co^{II} ions) at 300 K amounts to 4.37 μ_B (Figure 14), which is larger than the one expected for the spin-only[11, 12] case ($\mu_{\text{eff}} = 3.87\ \mu_B$, $S = 3/2$, $g = 2.0$). The μ_{eff} value of compound **2** decreases gradually to 4.04 μ_B at about 46 K and then decreases sharply to 1.13 μ_B at 2 K with cooling. The Curie–Weiss law is obeyed for **2** with a Curie constant of $C = 1.24\ \text{cm}^3\cdot\text{K}\cdot\text{mol}^{-1}$, $\theta = -9.79$ K. These results indicate a possible weak antiferromagnetic interaction in **2**.

The μ_{eff} value of complex **3** amounts to 2.27 μ_B at 300 K, and decreases smoothly to 2.05 μ_B at 41 K (Figure 15), which is much lower than the spin-only value for an uncoupled Ni^{II} ion ($\mu_{\text{eff}} = 2.83\ \mu_B$, $S = 1$, $g = 2.0$). The μ_{eff} value decreases rapidly from 41 K with cooling, reaches its minimum value of 0.55 μ_B at 2 K. The Curie–Weiss law is obeyed for compound **3** in the range of 14 to 300 K with a Curie constant of $C = 0.68\ \text{cm}^3\cdot\text{K}\cdot\text{mol}^{-1}$, $\theta = -16.83$ K. These results also indicate a possible weak antiferromagnetic interaction in **3**.

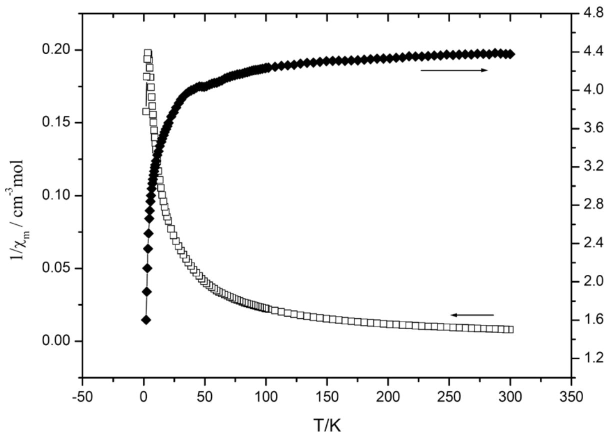

Figure 14. Plot of μ_{eff} and χ_M versus T for complex **2**.

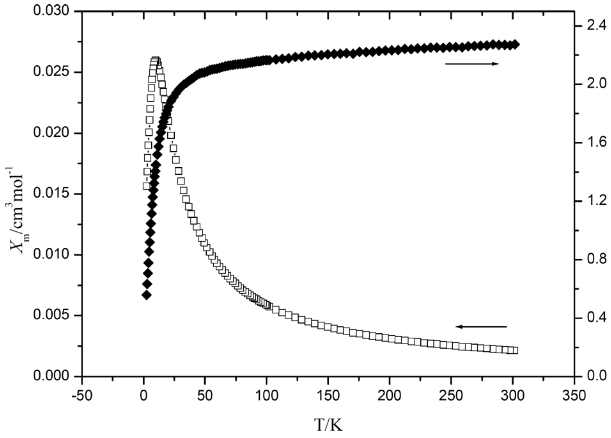

Figure 15. Plot of μ_{eff} andχ_M versus T for complex **3**.

Conclusions

Four new compounds based on PyBIm and terephthalate ligands, in which the weak interactions are important for construction of the compounds, were prepared and characterized. The successful preparation of the compounds further demonstrates that the PyBIm ligand is a good candidate for construction of new metal-organic complexes.

Acknowledgement

This work was financially supported by *Start-up Fund for Advanced Professional of Jiangsu University* (No. 08JDG031), and partly supported by *Industry High Technology Foundation of Jiangsu* (BG2007025).

References

[1] a) S. Kitagawa, K. Uemura, *Chem. Soc. Rev.* **2005**, *34*, 109; b) N. Tasios, C. Grigoriadis, M. R. Hansen, H. Wonneberger, C. Li, *J. Am. Chem. Soc.* **2010**, *132*, 7478; c) A. Pramanik, A. Basu, G. Das, *Polyhedron* **2010**, *29*, 1980; d) Y. B. Zhong, M. L. Cao, B. H. Ye, *Cryst. Growth Des.* **2008**, *8*, 2282; e) C. S. Liu, J. J. Wang, Z. Chang, L. F. Yan, *Z. Anorg. Allg. Chem.* **2009**, *636*, 1115.

[2] a) S. L. Ma, D. Zhang, S. Gao, Y. He, C. M. Qi, C. H. Fan, Y. F. Chen, X. J. Yang, *Eur. J. Inorg. Chem.* **2008**, 3776; b) B. M. Ji, S. B. Miao, D. S. Deng, C. X. Du, *Polyhedron* **2009**, *28*, 2611; c) G. Peng, Y. C. Qiu, Z. H. Liu, B. Liu, H. Deng, *Cryst. Growth Des.* **2010**, *10*, 114; d) J. G. Małecki, *Polyhedron* **2010**, *29*, 1237; e) Z. Y. Li, J. W. Dai, N. Wang, H. H. Qiu, S. T. Yue, Y. L. Liu, *Cryst. Growth Des.* **2010**, *10*, 2746.

[3] a) C. K. Xia, C. Z. Lu, D. Q. Yuan, Q. Z. Zhang, X. Y. Wu, J. J. Zhang, D. M. Wu, *J. Mol. Struct.* **2007**, *831*, 195; b) Z. Wang, S. R. Wilson, B. M. Foxman, W. Lin, *Cryst. Engineering* **1999**, *2*, 91; c) L. J. Chen, X. He, C. K. Xia, Q. Z. Zhang, J. T. Chen, W. B. Yang, C. Z. Lu, *Cryst. Growth Des.* **2006**, *6*, 2076.

[4] a) C. K. Xia, C. Z. Lu, X. Y. Wu, Q. Z. Zhang, J. J. Zhang, D. M. Wu, *Polyhedron* **2007**, *26*, 941; b) X. P. Lin, M. Pan, S. R. Zheng, Y. R. Liu, Q. T. He, B. S. Kang, C. Y. Su, *Cryst. Growth Des.* **2007**, *7*, 2481; c) C. K. Xia, C. Z. Lu, X. Y. Wu, L. J. Chen, Q. Z. Zhang, J. J. Zhang, D. M. Wu, *Inorg. Chim. Acta* **2006**, *359*, 4639; d) C. K. Xia, C. Z. Lu, Q. Z. Zhang, X. He, J. J. Zhang, D. M. Wu, *Cryst. Growth Des.* **2005**, *5*, 1569; M. X. Li, H. Wang, S. W. Liang, M. Shao, X. He, Z. X. Wang, S. R. Zhu, *Cryst. Growth Des.* **2009**, *11*, 4626.

[5] H. Wang, M. X. Li, M. Shao, X. He, *Polyhedron* **2007**, *26*, 5171.

[6] E. Alcalde, I. Dinares, L. Perez-Garcia, T. Roca, *Synthesis* **1992**, 395.

[7] G. M. Sheldrick, *SADABS*, University of Göttingen, Göttingen, Germany, **1996**.

[8] *SHELXTL* (version 5.05), Siemens Analytical X-ray Instruments Inc.: Madison, WI, **1994**.

[9] M. Tadokoro, K. Nakasuji, *Coord. Chem. Rev.* **2000**, *198*, 205.

[10] H. Wang, J. Getzschman, I. Senkovska, S. Kaskel, *Microporous Mesoporous Mater.* **2008**, *116*, 653.

[11] L. Carlin, *Magnetochemistry*, Springer-Verlag, New York, **1986**.

[12] E. Mabbs, D. J. Machin, *Magnetism and Transition Metal Complexes*, Oxford University Press, Oxford, **1973**.

Received: July 14, 2010